

See discussions, stats, and author profiles for this publication at: <https://www.researchgate.net/publication/231629202>

Synthesis of Thiolate-Stabilized Platinum Nanoparticles in Protolytic Solvents as Isolable Colloids

ARTICLE *in* THE JOURNAL OF PHYSICAL CHEMISTRY B · MAY 2001

Impact Factor: 3.3 · DOI: 10.1021/jp003779z

CITATIONS

96

READS

38

2 AUTHORS, INCLUDING:



Keisaku Kimura

Hosei University

186 PUBLICATIONS 3,728 CITATIONS

SEE PROFILE

Synthesis of Thiolate-Stabilized Platinum Nanoparticles in Protolytic Solvents as Isolable Colloids

Sihai Chen and Keisaku Kimura

Department of Material Science, Faculty of Science, Himeji Institute
of Technology, Harima Science Garden City, Kamigori,
Hyogo 678-1297, Japan

**The Journal of
Physical Chemistry B[®]**

Reprinted from
Volume 105, Number 23, Pages 5397–5403

Synthesis of Thiolate-Stabilized Platinum Nanoparticles in Protolytic Solvents as Isolable Colloids

Sihai Chen and Keisaku Kimura*

Department of Material Science, Faculty of Science, Himeji Institute of Technology,
Harima Science Garden City, Kamigori, Hyogo 678-1297, Japan

Received: October 13, 2000; In Final Form: January 24, 2001

Water-dispersible, isolable thiolate-stabilized platinum nanoparticles are synthesized by two one-phase methods: one is conducted in water; another mainly in methanol, through the reduction of chloroplatinic acid with sodium borohydride, using mercaptosuccinic acid (MSA) as the stabilizer. The well-separated particles with mean diameter of 2.5 nm are obtained in water when the initial molar ratio of MSA to chloroplatinic acid (S/Pt) is 0.7. High-resolution transmission electron microscopy reveals that most particles are fcc single crystals of cuboctahedral or truncated octahedral morphology with cell parameter similar to that of bulk Pt. The average particle diameter increases from 2.5 nm to around 4.7 nm upon decreasing the S/Pt ratio from 0.7 to 0.1; at the same time, particle aggregation occurs due to the incomplete coverage of thiolate molecules on the particle surface. The particles with mean diameter of 2.3 nm are also obtained while using methanol as the solvent at an initial S/Pt ratio of 0.5. Experiments through changing the concentration of sodium borohydride show that the reaction is thermodynamically controlled; the final Pt particle size is dictated by the initial S/Pt ratio.

Introduction

Metal nanoparticles have drawn increasing interest due to their novel properties, which are caused by size and surface effects and are different from those of bulk or molecular materials,¹ and due to their potential applications in catalysis² and nonlinear optics,³ and as electronic,⁴ magnetic,⁵ or other advanced⁶ materials. An important contribution to this area is the successful synthesis of long-chain thiolate-stabilized gold nanoparticles,⁷ which are air stable, isolable, and dispersible in organic solvent. These properties make it possible to prepare the monodispersed particles by fractional precipitation,⁸ or to store and manipulate the particles as stable solid and used for device applications. On the other hand, since long alkyl chains cover these particles, they are not dispersible in water. Hence, their applications in biological systems, which normally work in aqueous environments, are prevented. To overcome this problem, recently others⁹ and we¹⁰ have succeeded in the synthesis of water-dispersible thiolate-stabilized gold nanoparticles. We have also extended our method to the synthesis of silver nanoparticles.¹¹ As an extension of our ongoing work, in this report, we describe the synthesis of water-dispersible thiolate-stabilized platinum nanoparticles. Similar to the analogue of gold,¹⁰ these nanoparticles display good properties such as air stability, isolability, and redispersibility.

Platinum particles have been prepared previously using various stabilizers including polymers, ligands, and surfactants. If classified according to the active atoms of the functional groups in the molecules, these stabilizers can be (a) oxygen-containing, such as sodium citrate,¹² poly(vinyl alcohol),¹³ carbon monoxide,¹⁴ poly(ethylene glycol) monolaurate, and 10-undecenoic acid;¹⁵ (b) nitrogen-containing (in some cases also containing oxygen), such as tetraalkylammonium,^{13,16} poly(vinyl

pyrrolidone) (PVP),^{13,17} poly(methyl acrylate-*co*-N-vinyl-2-pyrrolidone),¹⁸ disodium 1,10-phenanthroline-4,7-bis(benzene-4-sulfonate),¹⁹ poly(*N*-isopropylacrylamide),²⁰ and *p*-aminobenzenesulfonate;²¹ (c) phosphorus-containing, such as polyphosphate²² and phosphine.^{14b} In contrast, sulfur-containing molecules such as thiolates have rarely been used directly for the synthesis of Pt nanoparticles. Based on the knowledge that thiolates can form monolayers on metallic platinum surfaces,²³ it is reasonable to infer that thiolates can also be used for the synthesis of platinum nanoparticles. In this regard, limited examples include the long-chain thiolate stabilized platinum²⁴ and gold–platinum alloy²⁵ nanoparticles, as well as 4-mercaptop-aniline²⁶ or per-6-thio- β -cyclodextrin²⁷ modified platinum particles. Different from these particles, the mercaptosuccinic acid modified platinum nanoparticles described in this paper possess the negatively charged carboxylate groups on their surface. Using a cationic surfactant tetraoctylammonium bromide (TOAB) as the phase-transfer agent, we find that the particles can be transferred into organic solvent such as toluene, benzene or diethyl ether. This is a remarkable property for the as-prepared nanoparticles, which differs from others. It shows that the nanoparticles can display the property similar to that of the anions if their surface is properly functionalized. Before this, phase transfer property is normally observed for anions, such as AuCl_4^- , etc.⁷

Experimental Section

Chemicals. Hydrogen hexachloroplatinate(IV) hexahydrate ($\text{H}_2\text{PtCl}_6 \cdot 6\text{H}_2\text{O}$, >98.5%), mercaptosuccinic acid ($\text{HOOCCH}_2\text{CH}(\text{SH})\text{COOH}$, 97%, denoted as MSA), methanol (99.8%), ethanol (99.5%) and other organic solvents were from Wako. Sodium borohydride (NaBH_4 , > 96%) was from Merck. All chemicals were used as received. Distilled water with resistance > 18.0 $\text{M}\Omega \cdot \text{cm}$ was used. All of the glassware and the Teflon-coated magnetic stirring beads were cleaned with *aqua regia*,

* Corresponding author. Fax: 81-7915-8-0161. Tel: 81-7915-8-0159.
E-mail: kimura@sci.himeji-tech.ac.jp

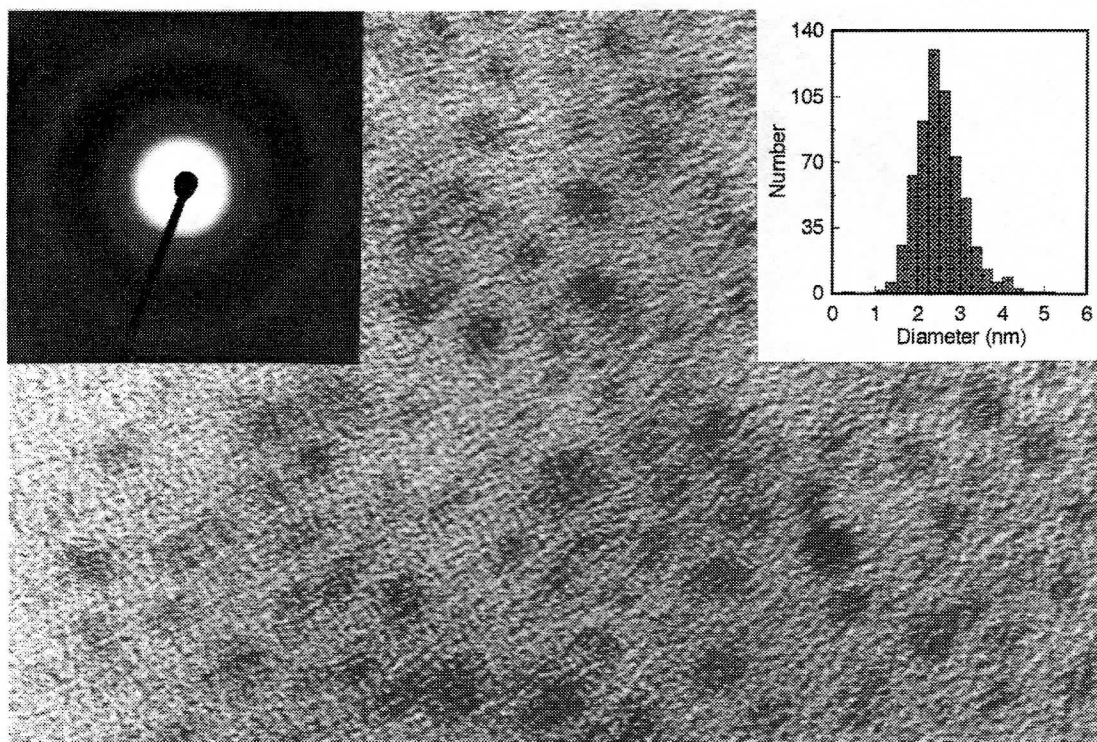


Figure 1. High-resolution TEM image of Pt nanoparticles prepared at S/Pt = 0.7 with method A. The inset shows the electron diffraction pattern and size distribution of particles.

followed by copious rinsing with warm tap water, doubly distilled water and dried in an oven.

Preparation of Pt Nanoparticles. Two methods, one is conducted in water (method A), another mainly in methanol (method B), were developed. They both include the addition of NaBH₄ aqueous solution (molar ratio between NaBH₄ and H₂PtCl₆ is fixed at 10 unless otherwise stated) into the freshly prepared mixture of MSA and H₂PtCl₆. A typical procedure of method A is as follows: 5 mL of 6.76×10^{-2} M NaBH₄ was added into the mixture of 10 mL of 3.38×10^{-3} M H₂PtCl₆ and 1 mL of 2.37×10^{-2} M MSA (molar ratio between MSA and H₂PtCl₆, S/Pt, equals 0.7) under vigorous stirring. The solution turned immediately from yellow to light brown, then gradually to deep brown resulting in the formation of 2.5 nm Pt nanoparticles.

The typical procedure of method B is an analogy that we developed for the preparation of gold nanoparticles with H₂PtCl₆ instead of HAuCl₄.¹⁰ After the reaction, the precipitates were separated, washed, and finally dried in a vacuum. Using this method, Pt nanoparticle powders were obtained while S/Pt ratios are 0.2 and 0.5.

Instrumentation and Characterization. Most instruments used have been described previously.^{10,28} Briefly; an Hitachi-8100 transmission electron microscope (TEM) was used to size the particles. Mean particle size and size distribution were obtained from the digitized photo images. X-ray diffraction (XRD) was performed on a Rigaku RINT/DMAX-2000 diffractometer with the X-ray generator (Cu K α radiation, $\lambda = 1.5418 \text{ \AA}$) operated at 40 kV and 20 mA. UV-vis absorption spectra of the samples were recorded on a Hitachi U-3210 spectrophotometer with 2 nm resolutions. Fourier transform infrared (FT-IR) spectra were recorded with a Horiba FT-210 infrared spectrophotometer using the KBr disk method. Thermo-gravimetry and differential thermoanalysis (TG/DTA) were performed on a fully computerized MAC 2000S system (MAC Sci Co.) at a heating rate of 10 °C per min in the temperature

range of 20–499 °C under a nitrogen flow of 40 mL per min. Elemental analyses of solid powders were conducted commercially at a chemical microanalytical laboratory of the Institute of Physical and Chemical Research, Japan, using standard techniques.

The solid powders before and after TG treatment were analyzed with an energy dispersive analyzer (EDA) DX-4 system attached to the Philips XL-20 scanning electron microscope (SEM) operated under an acceleration voltage of 9 kV. In this case, only the top of the thick sample, which was mounted on the SEM sampling stage with a double-sided conductive carbon tape, was focused in order to avoid the interference caused by the background tape.

Results and Discussion

Formation and Structure of Pt Nanoparticles. Figure 1 presents the high-resolution TEM photo of Pt nanoparticles prepared with method A at an S/Pt ratio of 0.7. The size distribution measured from these well-separated particles (total counting number $n = 611$), as shown in the inset of Figure 1, displays a mean (equivalent circle) particle diameter of 2.5 nm, with a relative standard deviation of 23%. The most frequently observed lattice fringes in the high-resolution image were 0.227 (± 5) and 0.196 (± 3) nm, which can be indexed to the lattice spacing of (111) and (200) planes of fcc Pt, respectively, indicating the formation of Pt particles. The electron diffraction pattern shown in the inset of Figure 1 displays two very diffusive rings: the small one covers the lattice fringes of the (111) and (200) planes of Pt, while the large one can be regarded as the combination of that of the (220), (311), and (222) planes. The diffusive nature of these rings is a characteristic indication of particles with sizes in the nanometer range.

Careful inspection revealed that the majority of particles possess structures based on apparently perfect fcc packing, with roughly regular or distorted hexagonal contours in projection

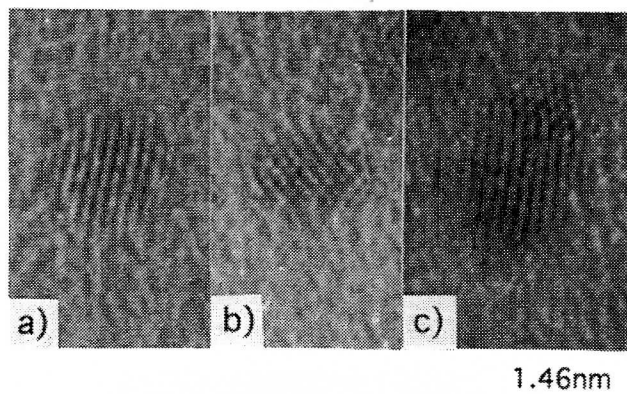


Figure 2. High-resolution TEM photos of (a) and (b), cubooctahedral or truncated octahedral, and (c) twined particles.

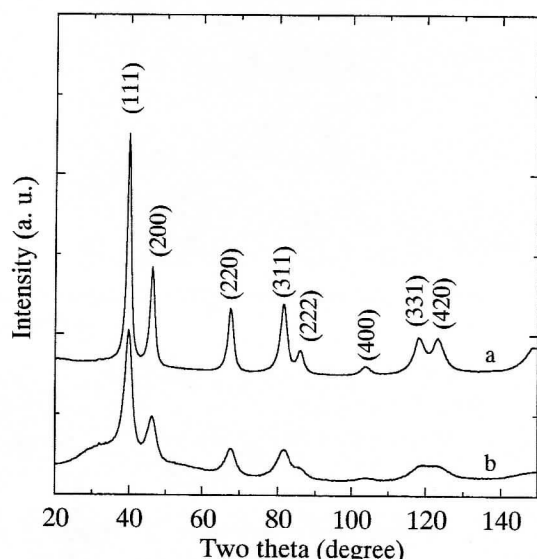


Figure 3. XRD patterns of the powders obtained with method B at initial S/Pt ratios of (a) 0.2 and (b) 0.5.

when viewed down a $\langle 110 \rangle$ direction (see Figure 2, a and b). This suggests a cubooctahedral or truncated octahedral morphology;⁸ the particle could be discernible as single crystal, because clear (111) or (200) lattice planes were observed to cover each whole particle. Occasionally, single twined particles were also observed (Figure 2c). Two viewpoints have been proposed to deduce the particle formation process from the structure of metal particles.²⁹ (a) If the structure of particles is similar to that of bulk, they are suggested to form through addition of atoms in normal metallic packing to final metallic structures. (b) If the small particles possess a multiple structure different from that of bulk fcc metal, they are often regarded as aggregates being produced by growth from stable nuclei (viz. tetrahedron). For example, perfect decahedral structures with 5-fold axes were observed for silver, and a polytetrahedral growth was proposed.²⁹ In the present case, we have not observed the decahedral or icosahedral morphology, implying that the growth through addition of Pt atoms with normal metallic packing to the fcc structure may take place in the early stages of particle formation.

Pt particle powders were also generated in methanol using method B when S/Pt ratios were 0.2 and 0.5 (see XRD patterns in Figure 3). TEM revealed that the particles prepared at S/Pt = 0.5 have a mean diameter of 2.3 nm with standard deviation of 0.71 nm. Elemental analysis gave (in %): Pt, 52; Na, 4.6; C, 8.9; H, 0.9; O, 18; S, 5.5. The atomic ratio of C:H:O:S is 4.0:4.9:6.1:0.9, indicating that in addition to the existence of

carboxylate (C:H:O:S is 4:3:4:1), water molecules are also included on the particle surface. This result is also supported by the FT-IR study: the spectrum of the nanoparticles (not shown) displayed a broad absorbance band peaked at 3482 cm^{-1} , which was caused by the summation of various O—H stretching vibrations. The amount of water was found to be 4.6% by thermogravimetric measurements. Comparing the FT-IR spectra of the pure MSA¹⁰ with that of the Pt particles, the S—H vibration peak of pure MSA at 2548 cm^{-1} is absent, indicating that MSA molecules combine with the Pt particle surface through an S atom and there is no remaining free MSA adsorbed on a particle surface. SEM—EDX analysis of the sample before and after TG treatment (heat to 499 °C) shows that after heating about 50–60% of the C or O element is lost, whereas only 20% of the sulfur lost. This implies that sulfur may combine tightly with Pt particle surface. The presence of double peaks at 1398 cm^{-1} (symmetric COO⁻ vibration) and 1578 cm^{-1} (asymmetric COO⁻ vibration) for the nanoparticles showed that MSA exists in the form of carboxylate salt. This result is similar to that of the MSA-modified gold nanoparticles.¹⁰

The surface structure of the Pt nanoparticles was further studied through a transference experiment. By shaking the Pt nanoparticle aqueous dispersion with toluene solution containing TOAB, the particles in water can be transferred into toluene without any aggregation as judged from TEM observation. This clearly confirmed that the surface of the Pt nanoparticles is negatively charged, consistent with the FT-IR result that MSA exists in the form of carboxylate salt. In recent reports,³⁰ we have elucidated the pure electrostatic interaction between carboxylate groups on the gold nanoparticle surface and positively charged TOAB through a similar transference experiment.

The above particle powders stored in an air-sealed bottle at ambient condition were found very stable, since no apparent size change was observed by TEM and XRD even after about 2 years. The existence and intensity of the two infrared peaks at around 1130 and 620 cm^{-1} , due to the ν_3 and ν_4 infrared-active modes of SO₄²⁻ anions, respectively, can be used as the criteria of chemical degradation of thiolate molecules.²⁶ These two peaks are not found for the freshly prepared nanoparticles and are very weak for the 2-year-aged samples, showing that MSA molecules have not been oxidized and combine tightly on the Pt particle surface. This is in drastic contrast to the 4-thioaniline stabilized Pt particles, which are very unstable and show complete degradation of the thioaniline on the particle surface within 4 months of aging.²⁶

Effect of S/Pt Ratio. The S/Pt ratio was found to be a critical parameter in controlling the generation of Pt nanoparticles. Figure 4 shows the absorption spectra of the 2-day-aged reaction solutions prepared with method A at S/Pt ratios of 0.1 to 2.4. As evident from the low absorbance at 600 nm (Figure 4 e-h), no particles were generated when S/Pt ≥ 1.14 . The produced solutions were transparent and showed colors from brown to yellow upon increasing the S/Pt ratios. When S/Pt ≤ 0.7 , the reacted solutions showed colors from deep-brown to black-brown with the decrease of the S/Pt ratios. The absorption spectra displayed a high absorbance at 600 nm and a gradual increase to the high energy, indicating the formation of Pt nanoparticles (Figure 4 a-d).^{12c}

The aggregation states of the Pt particles are also dependent on the S/Pt ratio. As shown in Figure 5, the particles aggregate severely at lower S/Pt ratios from 0.1 to 0.5. It is very difficult to exactly measure the particle size under these conditions, but a rough estimation gave that the particle size increased slightly

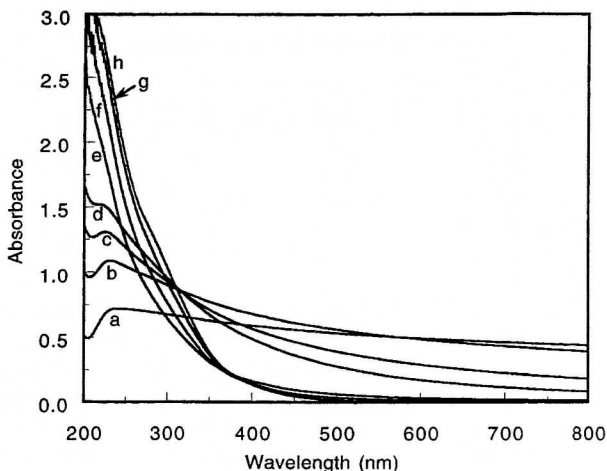


Figure 4. The absorption spectra of reaction mixtures prepared with method A at different initial S/Pt ratios: (a) 0.10, (b) 0.31, (c) 0.50, (d) 0.70, (e) 1.14, (f) 1.61, (g) 2.09, and (h) 2.40. The spectra were recorded 2 days after the reaction. The concentration of H_2PtCl_6 and NaBH_4 are 2.11×10^{-3} M and 2.11×10^{-2} M, respectively. The spectra were measured with samples of 10 times dilution with water.

as the S/Pt ratio decreased (see Table 1). Constructing a double-logarithmic plot of diameter, D (nm), versus the MSA concentration, c (M), we found $\log D = a + b \log c$ with $a = 0.40$ and $b = 0.33$. Since the aggregation number of Pt atoms is

TABLE 1: Microscopic Parameters of the Platinum Sol Prepared by Method A at Different S/Pt Ratios

S/Pt	code ^a	mean diameter (nm)	relative standard deviation (%)	counting number	theoretical S/Pt ^b
0.1	a	4.7	27	407	0.14
0.3	b	3.7	26	507	0.18
0.5	c	3.4	31	423	0.19
0.7	d	2.5	23	611	0.26

^a Spectrum code shown in Figure 4. ^b Theoretical S/Pt ratios for different sized particles assuming that thiolate molecules form self-assembled monolayer on the particle surface with a packing density of 14 \AA^2 .²⁶

proportional to the cube of particle diameter, the aggregation number of Pt particle decreases with 0.99th power of the MSA concentration. This power is about half the value that was observed in the case of gold,¹⁰ showing a lower ability of thiolate to terminate the growth of Pt than that of gold, probably due to the weaker interaction strength between Pt and thiolate.^{23b}

The aggregation of Pt particles has been observed when citrate or polymer is used as the stabilizer,¹² but it is difficult to explain the reason due to the difficulty in defining the surface structure of particles. In the present case, because thiolate molecules can form a monolayer on the Pt particle surface through head-on S atom, we propose that the aggregation may be due to the incomplete coverage of thiolate molecules on the particle surface, the bare particle surfaces acting as the connecting points

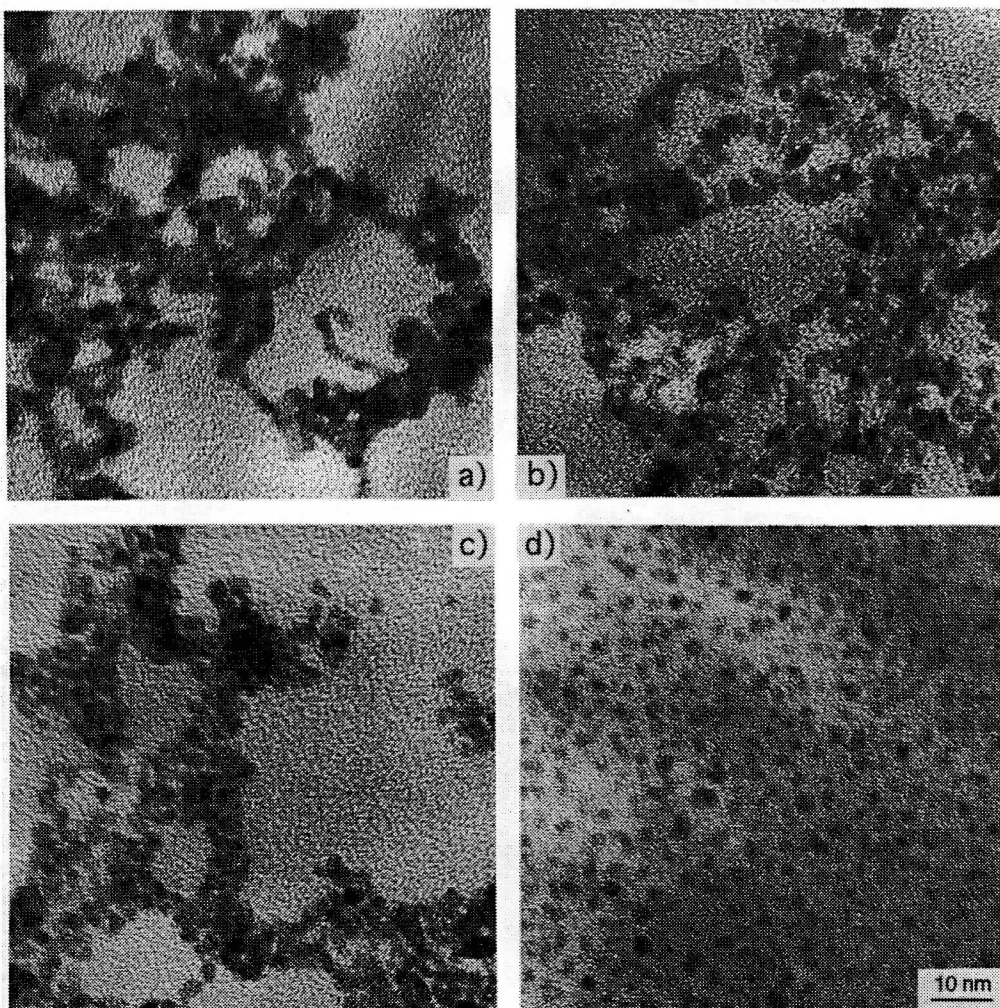


Figure 5. TEM photos of the Pt particles prepared at S/Pt ratios of (a) 0.10, (b) 0.31, (c) 0.50, and (d) 0.70. Other conditions are the same as in Figure 4. The scale bar applies to all four photos.

between particles. According to the calculated theoretical S/Pt ratios required for a full monolayer coverage as shown in Table 1, when S/Pt = 0.1 the amount of thiolate is indeed not enough to fully cover the particle surface. When S/Pt = 0.3 and 0.5, the amount of thiolate is found enough to fully cover the particle surface. In these cases, the aggregation may be due to desorption of thiolate molecules from the particle surface caused by particle collision or other reasons. It is only when S/Pt = 0.7 that the aggregation can be completely inhibited (Figure 5d).

Effect of NaBH₄ Concentration. To further understand the particle nucleation and growth processes, we have studied the effect of NaBH₄ concentration on the sizes of the resultant particles. As we know, many mechanisms have been proposed to account for particle formation processes. For example, a diffusion-controlled growth model has been elucidated for the synthesis of monodispersed particles.³¹ Recent experiments also showed that many uniform particles are formed through the aggregation of small subunits, which is documented as an aggregation mechanism.³² In the case of thiolate-stabilized gold nanoparticles,³³ due to the strongly adsorbed thiolate monolayer on the particle surface, the reaction model has been demonstrated to be thermodynamically controlled.³³ Characteristic of such a process is that the final particle size is controlled solely by the initial molar ratio of reactants. Considering the similar characteristics obtained in the present work as shown in the last section, it is reasonable to propose that a thermodynamically controlled reaction process may be the case of the present study. To distinguish this mechanism from the former two, an important experiment, i.e., to increase the supersaturation of the precursor atoms used for particle formation while keeping the S/Pt ratio the same, should be done. In the former two mechanisms, the particle size would increase due to the growth or aggregation, whereas in the thermodynamic case, the particle size should not change.

To increase the supersaturation of the precursor atoms, the NaBH₄ concentration was increased gradually while keeping the S/Pt ratio constant at 0.7. From the 500-nm absorbance change as shown in Figure 6, the reduction and particle formation process ended at about 3 h after the reaction. The 500-nm absorbance for the stable sols (24 h after the reaction) was found to be linearly proportional to the concentrations of NaBH₄ (Figure 7), indicating that the total reduced amount of platinum increased as the amount of the reducing agent increased. TEM observation revealed that the particle sizes are almost the same under different NaBH₄ concentrations (Table 2). This demonstrates that the increase in absorbance at 500 nm is caused by the increased amount of Pt nanoparticles of the same particle size, i.e., the increase in the supersaturation of the precursor atoms cannot result in larger particles or aggregation of particles, and the particle size is controlled by the initial S/Pt ratio. These results clearly support that the formation of thiolate-modified Pt nanoparticles is a thermodynamically controlled reaction process, similar to that of the thiolate-stabilized gold nanoparticles.³³

Optical Properties. Colloidal dispersions of metals display absorption in the UV-vis region, these are caused by the excitation of plasmon resonance or interband transition and thus are characteristic properties of metals. Based on the calculations by Creighton et al.³⁴ for the 10 nm particle according to the classic Mie theory,³⁵ Pt particles are expected to exhibit a weak absorption band at 215 nm, the position of which is independent of the particle size in the range of 3–20 nm. This band has indeed been observed for different-sized Pt particles prepared by radiolytic and chemical reduction of PtCl₆²⁻ (1.8 and 7 nm),²²

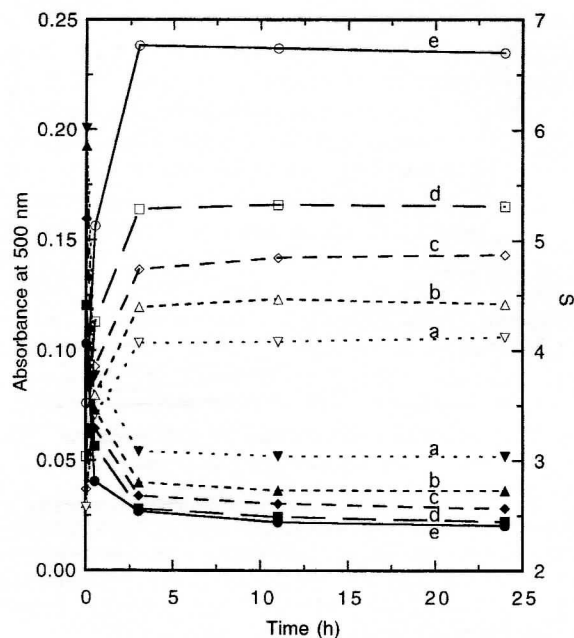


Figure 6. The effect of NaBH₄ concentration on the optical properties of the Pt sols. The empty points represent the absorbance at 500 nm, the filled points show the S value. See text for further explanation. The particles were prepared with standard condition of method A at S/Pt = 0.7. The concentration of NaBH₄ are (a) 0.001 M, (b) 0.002 M, (c) 0.005 M, (d) 0.01 M, and (e) 0.02 M. The optical spectra were recorded samples of 10 times dilution with water.

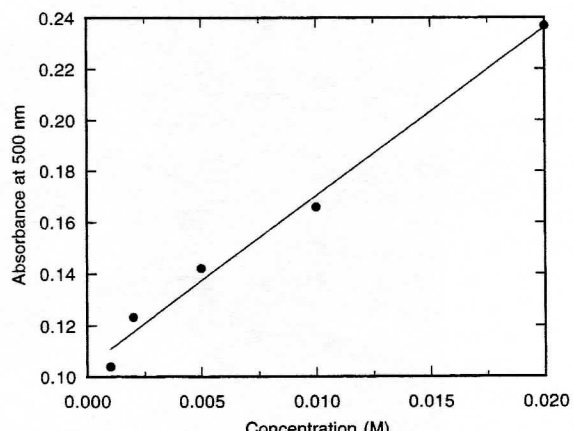


Figure 7. The change of the absorbance at 500 nm of the final stable Pt sols (after 24 h of aging) with the concentration of NaBH₄. Other conditions were the same as in Figure 6.

TABLE 2: Microscopic Parameters of the 24-Hour-Aged Platinum Sols Prepared at S/Pt = 0.7 by Method A with Different Molar Ratios of [NaBH₄]/[H₂PtCl₆]

[NaBH ₄]/[H ₂ PtCl ₆]	mean diameter (nm)	relative standard deviation (%)	counting number
10	2.5	23	611
5.0	2.3	28	416
2.5	2.7	26	303
1.0	2.4	21	391
0.5	2.3	26	237

or ethanol reduction of PtCl₆²⁻ in the presence of poly(*N*-isopropylacrylamide) (2.3 nm).²⁰ We have also observed the similar peak here from the 2-day-aged Pt sols (Figure 4, curves a-d). However, the maximum shifted from 218 to 235 nm, along with the broadening of the band as the S/Pt ratio changed from 0.7 to 0.1. Moreover, in all cases this band faded away after further aging to 5 days. Besides the change of particle sizes, the peak shift and width change of the plasmon band may

TABLE 3: Optical Parameters *S* of the Platinum Sol Prepared by Method A at Different S/Pt Ratios during Aging

aging time	S/Pt			
	0.1	0.3	0.5	0.7
1 hour	1.36	2.28	2.73	2.96
2 days	0.44	0.83	1.64	2.57
5 days			1.58	2.33
5 months			1.52	2.35

be caused by the change in the conduction electron density³⁶ or the dielectric function³⁷ of metal particles, but in our case, according to the TEM observation shown in Figure 5, it is plausible to attribute this red shift to the aggregation of particles, which is mainly caused by the strong dipole-dipole interaction in the aggregates.³⁸ The disappearance of the plasmon band of Pt particles after longer time of aging implies that this band may be sensitive to the surface properties of the particles. As we know, Pt has a strong affinity for oxygen,^{23b} aging in air may have resulted in the oxidation of surface Pt atoms.

The optical properties of the Pt sols have been depicted using a parameter *S* ($S = -d(\log \text{extinction})/d(\log \text{wavelength})$) derived by Furlong et al.^{12c} This value was found to decrease with the decrease in S/Pt ratio (Table 3), consistent with the discussion that *S* values decreased with a stronger aggregation, and, in turn, a decrease in particle sphericity of the platinum sol.^{17b} On the other hand, in the experiments of Figure 6, at the initial particle formation steps, the *S* values were found to decrease with the particle growth, i.e., *S* values are related to the particle size. By comparing the final *S* values at different NaBH₄ concentrations, *S* values were found to decrease at a higher NaBH₄ concentration. Since the particle sizes under these conditions are almost the same (Table 2), these decreases should be related to the increased particle concentrations. This shows that the *S* value is a complex parameter affected by several factors including size, morphology, aggregation state, and even particle concentration.

Conclusion

Water-dispersible platinum nanoparticles have been successfully synthesized by the reduction of chloroplatinic acid in the presence of mercaptosuccinic acid. Because these particles are stabilized by thiolate, they possess good properties including air stability, isolability, and redispersibility. The well-separated fcc single crystal particles of 2.5 nm are obtained in water when initial molar ratio of mercaptosuccinic acid to Pt (S/Pt) is 0.7. The average particle diameter can be changed to 4.7 nm by decreasing the S/Pt ratio to 0.1; at the same time, particle aggregation occurs due to the incomplete coverage of thiolate molecules on the particle surface. The particle formation process is found to be a thermodynamically controlled process.

Acknowledgment. This work was supported in part by Grants-in-Aid for Scientific Research on Basic Research (A: 09304068) and for JSPS fellows from Ministry of Education, Science, Sports and Culture, Japan. S.C. thanks the Japan Society for Promotion of Science for granting the postdoctoral fellowship. We thank the help from Prof. K. Toriumi and Dr. Y. Ozawa in thermogravimetric analysis.

References and Notes

- (a) Henglein, A. *Chem. Rev.* **1989**, *89*, 1861. (b) Schmid, G. *Chem. Rev.* **1992**, *92*, 1709. (c) Mulvaney, P. *Langmuir* **1996**, *12*, 788.
- (a) Bradley, J. S. In *Clusters and Colloids, From Theory to Application*; Schmid, G., Ed.; VCH: Weinheim, 1994; Chapter 6, p 459.
- (b) Schmid, G.; Maihack, V.; Lantermann, F.; Peschel, S. *J. Chem. Soc., Dalton Trans.* **1996**, 589.
- (a) Olsen, A. W.; Kafafi, Z. H. *Proc. Mater. Res. Soc. Symp.* **206**; Materials Research Society: Pittsburgh, 1991; p 175. (b) Chen, S.; Nickel, U. *J. Chem. Soc., Chem. Commun.* **1996**, *133*. (c) Chen, S.; Nickel, U. *J. Chem. Soc., Faraday Trans. I* **1996**, *92*, 1555.
- (d) Schon, G.; Simon, U. *Colloid Polym. Sci.* **1995**, *273*, 101; 202.
- (e) Osuna, J.; de Caro, D.; Amiens, C.; Chaudret, B.; Snoeck, E.; Respaud, M.; Broto, J.; Fert, A. *J. Phys. Chem.* **1996**, *100*, 14571. (f) de Caro, D.; Ely, T. O.; Mari, A.; Chaudret, B.; Snoeck, E.; Respaud, M.; Broto, J.; Fert, A. *Chem. Mater.* **1996**, *8*, 1987.
- (g) Andres, M. P.; Ozin, G. A. *Chem. Mater.* **1989**, *1*, 174.
- (h) Brust, M.; Walker, M.; Bethell, D.; Schiffrian, D. J.; Whynes, R. *J. Chem. Soc., Chem. Commun.* **1994**, *801*.
- (i) Whetten, R. L.; Khouri, J. T.; Alvarez, M. M.; Murthy, S.; Vezmar, I.; Wang, Z. L.; Stephens, P. W.; Cleveland, C. L.; Luedtke, W. D.; Landman, U. *Adv. Mater.* **1996**, *8*, 428.
- (j) Schaaff, T. G.; Knight, G.; Shafiqullin, M. N.; Borkman, R. F.; Whetten, R. L. *J. Phys. Chem. B* **1998**, *102*, 10643. (k) Templeton, A. C.; Chen, S.; Gross, S. M.; Murry, R. C. *Langmuir* **1999**, *15*, 66.
- (l) Chen, S.; Kimura, K. *Langmuir* **1999**, *15*, 1075.
- (m) Chen, S.; Kimura, K. *Chem. Lett.* **1999**, *1169*.
- (n) (a) Aika, K.; Ban, L. L.; Okura, I.; Namba, S.; Turkevich, J. *J. Res. Inst. Catal.*, Hokkaido University **1976**, *24*, 54. (b) Brugger, P.; Cuendet, P.; Gratzel, M. *J. Am. Chem. Soc.* **1981**, *103*, 2923. (c) Furlong, D. N.; Launikonis, A.; Sasse, W. H. F.; Sanders, J. V. *J. Chem. Soc., Faraday Trans. I* **1984**, *80*, 571. (d) Turkevich, J.; Miner, R. S., Jr.; Babenkova, L. *J. Phys. Chem.* **1986**, *90*, 4765.
- (o) (a) Hirai, H.; Nakao, Y.; Toshima, N. *J. Maromol. Sci. Chem.* **1979**, *A13*, 727. (b) Delcourt, M. O.; Keghouche, N.; Belloni, J. *Nouv. J. Chem.* **1983**, *7*, 131.
- (p) (a) Chini, P. *J. Organomet. Chem.* **1980**, *200*, 37. (b) Fujimoto, T.; Fukuoka, A.; Iijima, S.; Ichikawa, M. *J. Phys. Chem.* **1993**, *97*, 279. (c) Rodriguez, A.; Amiens, C.; Chaudret, B.; Casanove, M.-J.; Lecante, P.; Bradley, J. S. *Chem. Mater.* **1996**, *8*, 1978. (d) Henglein, F. A. *J. Phys. Chem. B* **1997**, *101*, 5889.
- (q) Toshima, N.; Takahashi, T. *Bull. Chem. Soc. Jpn.* **1992**, *65*, 400.
- (r) (a) Boutonnet, M.; Kizling, J.; Stenius, P.; Maire, G. *Colloids Surf.* **1982**, *5*, 209. (b) Toshima, N.; Takahashi, T.; Hirai, H. *Chem. Lett.* **1985**, 1245. (c) Bonnemann, H.; Brioux, W.; Brinkmann, R.; Dinjus, E.; Joussen, T.; Korall, B. *Angew. Chem., Int. Ed. Engl.* **1991**, *30*, 1312. (d) Yonezawa, T.; Tominaga, T.; Toshima, N. *Langmuir* **1995**, *11*, 4601. (e) Reetz, M. T.; Quaiser, S. *Angew. Chem., Int. Ed. Engl.* **1995**, *34*, 2240. (f) Bonnemann, H.; Braun, G. A. *Angew. Chem., Int. Ed. Engl.* **1996**, *35*, 1992. (g) Reetz, M. T.; Winter, M.; Dimpich, G.; Lohau, J.; Friedrichowski, S. *J. Am. Chem. Soc.* **1997**, *119*, 4539.
- (h) Hirai, H. *J. Maromol. Sci. Chem.* **1979**, *A13*, 633. (i) Duff, D. G.; Edwards, P. P.; Johnson, B. F. G. *J. Phys. Chem.* **1995**, *99*, 15934.
- (j) Ohtaki, M.; Toshima, N.; Komiyama, M.; Hirai, H. *Bull. Chem. Soc. Jpn.* **1990**, *63*, 1433.
- (k) Schmid, G.; Morun, B.; Malm, J. *Angew. Chem., Int. Ed. Engl.* **1989**, *28*, 778.
- (l) Chen, C.-W.; Akashi, M. *Langmuir* **1997**, *13*, 6465.
- (m) Schmid, G.; Lehnert, A.; Malm, J.; Bovin, J. *Angew. Chem., Int. Ed. Engl.* **1991**, *30*, 852.
- (n) Henglein, A.; Ershov, B. G.; Malow, M. *J. Phys. Chem.* **1995**, *99*, 14129.
- (o) Hickman, J. J.; Laibinis, P. E.; Auerbach, D. I.; Zou, C.; Gardner, T. J.; Whitesides, G. M.; Wrighton, M. S. *Langmuir* **1992**, *8*, 357. (p) Shimazu, K.; Sato, Y.; Yagi, I.; Uosaki, K. *Bull. Chem. Soc. Jpn.* **1994**, *67*, 863.
- (q) Yee, C.; Scotti, M.; Ulman, A.; White, H.; Rafailovich, M.; Sokolov, J. *Langmuir* **1999**, *15*, 4314.
- (r) Hostettler, M. J.; Zhong, C.; Yen, B. K. H.; Anderegg, J.; Gross, S. M.; Evans, N. D.; Porter, M.; Murray, R. W. *J. Am. Chem. Soc.* **1998**, *120*, 9396.
- (s) Perez, H.; Pradeau, J.-P.; Albouy, P.-A.; Perez-Ornil, J. *Chem. Mater.* **1999**, *11*, 3460.
- (t) Alvarez, J.; Liu, J.; Roman, E.; Kaifer, A. E. *J. Chem. Soc., Chem. Commun.* **2000**, 1151.
- (u) Chen, S.; Ida, T.; Kimura, K. *J. Phys. Chem. B* **1998**, *102*, 6169.
- (v) Duff, D. G.; Curtis, A. C.; Edwards, P. P.; Johnson, B. F. G.; Logan, D. E. *J. Chem. Soc., Chem. Commun.* **1987**, 1264.
- (w) Yao, H.; Momozawa, O.; Hamatani, T.; Kimura, K. *Bull. Chem. Soc. Jpn.* **2000**, *73*, 2675. (x) Chen, S.; Yao, H.; Kimura, K. *Langmuir* **2001**, *17*, 733.
- (y) LaMer, V. K.; Dingar, R. H. *J. Am. Chem. Soc.* **1950**, *72*, 4847.
- (z) Turkevich, J.; Stevenson, P. C.; Hillier, J. *Faraday Discuss. Chem. Soc.* **1951**, *11*, 55. (aa) Reiss, H. *J. Chem. Phys.* **1951**, *19*, 482. (bb) Murray, C. B.; Norris, D. J.; Bawden, M. G. *J. Am. Chem. Soc.* **1993**, *115*, 8706. (cc) Sugimoto, T.; Chen, S.; Muramatsu, A. *Colloids Surf. A* **1998**, *135*, 207.
- (dd) Lee, S. H.; Her, Y. S.; Matijevic, E. *J. Colloid Interface Sci.* **1997**, *186*, 193.

- (33) (a) Leff, D. V.; Ohara, P. C.; Heath, J. R.; Gelbart, W. M. *J. Phys. Chem.* **1995**, *99*, 7036. (b) Whetten, R. L.; Gelbart, W. M. *J. Phys. Chem.* **1994**, *98*, 3544.
- (34) Creighton, J. A.; Eadon, D. G. *J. Chem. Soc., Faraday Trans. 1* **1996**, *87*, 3881.
- (35) Look, D. C. *J. Colloid Interface Sci.* **1976**, *56*, 386.
- (36) Henglein, A.; Mulvaney, P.; Linnert, T. *Faraday Discuss.* **1991**, *92*, 31.
- (37) Torigoe, K.; Nakajima, Y.; Esumi, K. *J. Phys. Chem.* **1993**, *97*, 8304.
- (38) Quinten, M.; Schonauer, D.; Kreibig, U. *Z. Phys. D* **1989**, *12*, 521.